



Evaluating low impact development practices potentials for increasing flood resilience and stormwater reuse through lab-controlled bioretention systems

Marina Batalini de Macedo ^{a,*}, Thalita Raquel Pereira de Oliveira^a, Tassiana Halmenschlager Oliveira^a, Marcus Nóbrega Gomes Junior^{a,b}, José Artur Teixeira Brasil^a, Cesar Ambrogi Ferreira do Lago^{a,b} and Eduardo Mario Mendiondo ^c

^a Hydraulic Engineering and Sanitation, University of São Paulo, Av. Trabalhador Saocarlense, 400 CP 359 São Carlos, SP CEP 13566-590, Brazil

^b University of Texas at San Antonio, One UTSA Circle, San Antonio, TX 78249, USA

^c University of São Paulo, Av. Trabalhador Saocarlense, 400 CP 359 São Carlos, SP CEP 3566-590, Brazil

*Corresponding author. E-mail: marinabatalini@usp.br

 MBM, 0000-0003-2829-754X

ABSTRACT

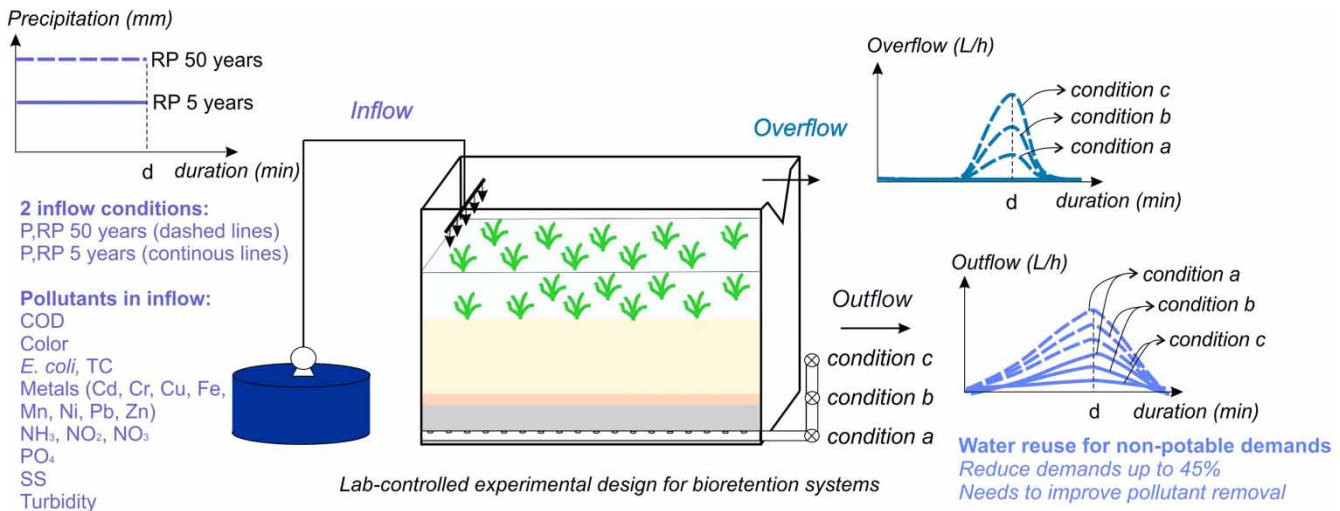
Low impact development practices (LID) as alternative measures of urban drainage can be used within the approach of resources recycling and co-management. This study evaluates the potential contribution of a bioretention system to flood control, non-potable water demands (NPD) and resources co-management. Bioretention setups were tested experimentally under variable conditions to identify operational key-factors to multiple purposes. Additionally, the efficiencies obtained for laboratory scale were extrapolated for household and watershed scale, quantifying the indicators of water demand reduction (WDR), energy demand reduction (EDR) and carbon emission reduction (CER) for hybrid systems with LID. The laboratory results indicated that the use of a bioretention with a submerged zone can improve the quality of the water recovered for reuse, while maintaining the efficiency of runoff retention and peak flow attenuation. Comparing the bioretention effluent quality with the Brazilian standards for stormwater reuse, the parameters color, turbidity, *E. coli* and metals were above the limits, indicating the necessity of a better treatment for solids particles and disinfection. Expanding the analysis to watershed scale, the bioretention helped to reduce NPD demands up to 45%, leading to a reduction in energy demand and carbon emission from the centralized water supply system.

Key words: exploratory analysis, low impact development, nature-based solutions, runoff retention, water-energy-greenhouse gases nexus, water quality

HIGHLIGHTS

- Bioretention prototype is evaluated for flood resilience and non-potable water demands.
- Bioretention setups are tested under variable rainfall, soil saturation and head losses.
- Water reuse for non-potable demands require better pollutant removal rates.
- Stormwater harvesting decreases water stress, energy demands and carbon emission.
- Monetary savings through stormwater harvesting were obtained.

GRAPHICAL ABSTRACT



1. INTRODUCTION

The United Nations Conference on Sustainable Development (also known as Rio +20) discussed the challenges to achieve sustainable development worldwide. The need for a new agenda (2030 agenda) was established, in which the 17 Sustainable Development Goals (SDG) were presented to be delivered until 2030, with a growing concern regarding climate change and its consequences (UN 2020). Studies suggest that global climate change is increasing local hydrological extremes (IPCC 2007; Hansen *et al.* 2010), creating additional challenges for water management. Carter *et al.* (2015) and Miller & Hutchins (2017) found an intensification of dry summers and rainy winters for regions of the United Kingdom. Similar results were found by Liuzzo *et al.* (2015) and Arnone *et al.* (2013) for Italy, where, despite the annual reduction trend in precipitation, torrential rainfall events increase and become more frequent. For the Brazilian megacities São Paulo and Rio de Janeiro, Lyra *et al.* (2018) obtained total rainfall reductions of 40 and 50%, respectively, during the rainy season. The reduction in the rainfall volume has great impact on the water, energy and food security of the population. The region of São Paulo experienced a near collapse of water supply and energy systems between 2014 and 2016, due to a period of extreme drought (Escobar 2015; Tafarello *et al.* 2016), which begins to repeat in the year of 2021. At the same time, there is also a trend of increasing heavy rainfall events in these regions (Chou *et al.* 2014). These studies demonstrate that problems related to flooding and water insecurity will be intensified and suffered even in the same locality.

In the 2030 agenda and their SDGs, urgent actions to fight climate change and adapt society to its impacts were pointed out, such as strengthening resilience and the capacity to adapt to climate-related risks in different locations; institutional and human capacity in mitigation, adaptation and reduction of impacts; and targets for reducing carbon emissions by the signatory countries (UN 2020; UNSTATS 2020). In addition, the high rate of urbanization leads to an increase in pavement areas and high population density, dropping local resilience to rainfall extremes in the cities (Carter *et al.* 2015). In 2014, the world's 40 largest cities (C40 group)¹ launched a diagnostic and evaluation report of its proposed actions. In this report C40 & ARUP (2014), 90% of the cities of the group indicated that climate change presents significant risks to their localities, the majority is associated with floods and water stress. Furthermore, urban drainage was pointed as a key to flood risk management, in which alternative urban drainage systems occupied the third place in the actions most performed by the group. Therefore, the importance of urban drainage as adaptation measures to make cities more resilient is noted.

Alternative urban drainage, known as low impact development (LID) practices,² initially aimed to reintegrate runoff excess into the hydrological cycle, by increasing the infiltration, decreasing runoff velocity, and reducing pollutant loads

¹ Currently, the C40 has 96 affiliated cities.

² These systems are also known as Sustainable Urban Drainage Systems (SUDS), Water Sensitive Urban Design (WSUD), Sponge cities, Best Management Practices (BMP), Compensatory Techniques (CT), depending on the location.

(Fletcher *et al.* 2013). These techniques can also be applied in a decentralized manner, prioritizing the runoff control at the source (Fletcher *et al.* 2015; Eckart *et al.* 2017). Although its initial purposes were runoff control, to re-establish the natural hydrological cycle, and to reduce pollution in urban rivers, new studies have been developed based on systemic approaches, such as the *water-energy-food nexus* (Macedo *et al.* 2021) and *water-energy-greenhouse gases nexus* (Nair *et al.* 2014), integrating mitigation and adaptation measures to the LID practices. Some examples are rainwater and stormwater harvesting (runoff recycling) for non-potable uses (Burns *et al.* 2015; Chandrasena *et al.* 2016; Petit-Boix *et al.* 2018; Freni & Liuzzo 2019), food cultivation (Richards *et al.* 2015; Ng *et al.* 2018), nutrient recycling (Ge *et al.* 2016), production and/or reduction of energy demands (Hashemi *et al.* 2015) and carbon sequestration (Getter *et al.* 2009; D'Acunha & Johnson 2019; Charalambous *et al.* 2019). From these cycles, 3rd generation LID has the capacity to contribute to SDG 2 – zero hunger, SDG 6 – clean water and sanitation, SDG 7 – affordable and clean energy, SDG 11 – sustainable cities and communities, SDG 13 – climate action (Macedo *et al.* 2021), and their respective targets in urban centers via different pathways (Figure 1), which can be evaluated with metrics and indicators on a local scale. The use of LID practices to meet SDGs is based on the phrase ‘Think globally, act locally’, increasingly used in the lexicon of sustainable development (Charlesworth 2010).

This study aims to present an initial and integrated assessment of how bioretention systems can contribute to the SDGs, by evaluating experimentally a bioretention device in laboratory scale and proposing evaluation metrics to quantify the resources recycling and co-management in the watershed. Main focus is given to flood control and resilience (runoff retention and peak flow attenuation), water reuse by stormwater harvesting to meet non-potable demands, resources co-management by hybrid water supply and drainage systems, and reductions in energy demand and carbon emission, therefore contributing at local scale to SDGs 6, 11 and 13. To this end, this study is separated into two main stages: (1) exploratory data analysis of water balance and water quality of a bioretention system in laboratory scale, in order to identify the most suitable configurations for optimization of resources recycling; (2) extrapolation of the results to watershed scale aiming to quantify the bioretention contribution to SDGs 6, 11 and 13 by local indicators.

2. MATERIALS AND METHODS

2.1. Investigation of bioretention performance through laboratory-controlled events

2.1.1. System of study and description of monitored events

In this study, a laboratory prototype of a bioretention system was evaluated (Figure 2), representing a real system at property scale. The field system collects water drained from a roof of 94 m², located on Campus 2 of the University of São Paulo, situated in the Mineirinho watershed, in the city of São Carlos, SP, Brazil (Gomes Junior 2019). The laboratory prototype was

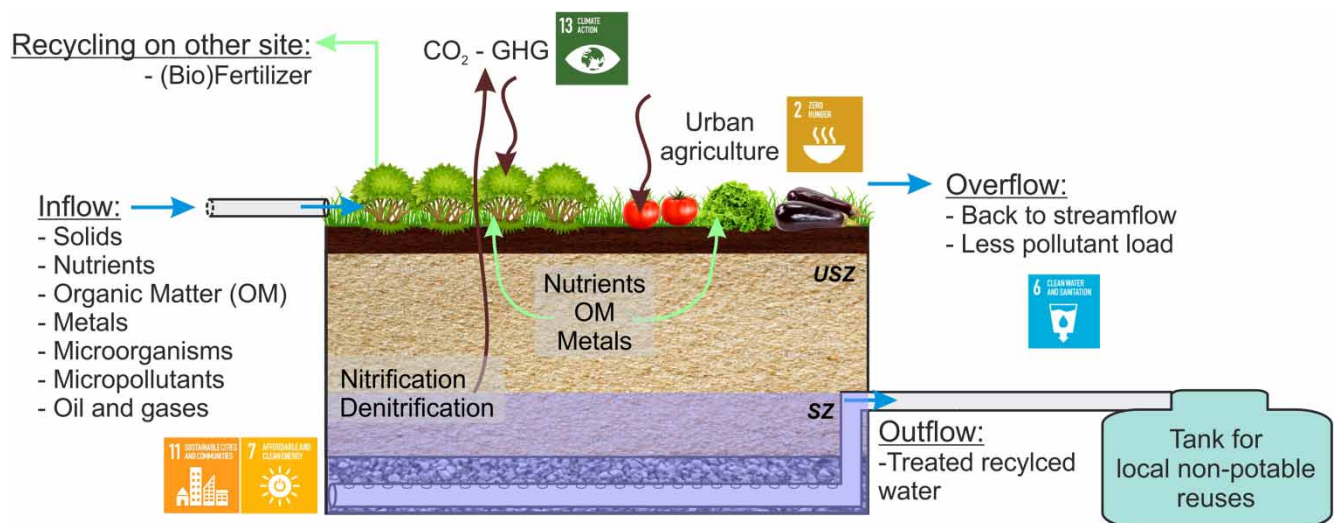


Figure 1 | Resource recycling pathways in a lined bioretention aiming at Sustainable Development Goals (SDGs). In the figure, USZ represents the unsaturated zone and SZ represents the saturated zone, the blue arrows represent the runoff pathways, the brown arrows represent the carbon pathways, and the green arrows represent the nutrient pathways through plant uptake.

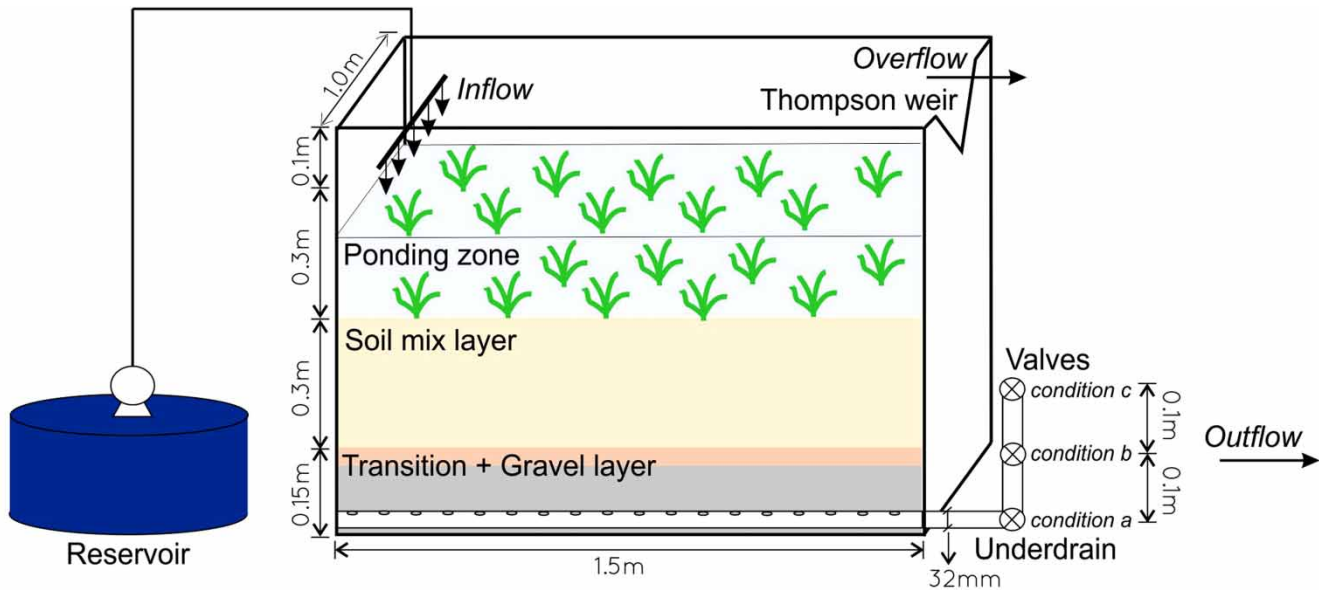


Figure 2 | Bioretention box scheme: the filtering medium is composed of 20% of natural soil and 80% of coarse sand, and drainage medium is formed by medium of medium-sized gravel.

made on a 1:2 scale with the field system. The daily precipitation that occurs at 90% frequency (P90) for the city is 32.5 mm. More details of the climate are provided in Supplementary Material (SM1).

The laboratory prototype was built in the form of a bioretention box (Davis *et al.* 2006; Macedo *et al.* 2018) and it is located in an open and ventilated but covered shed. The use of the bioretention box and its installation site aimed to reduce incomparable conditions in the climate (mainly temperature and humidity) and minimize the effects of different boundary conditions (unrealistic conditions were noted as one of the problems in LID studies and advances, according to Sambito *et al.* (2021)). The bioretention box allows keeping physical similarities as close as possible to the real system in the field to ensure that the hydraulic and treatment processes that occur are replicated in the laboratory. In this regard, the scale of 1:2 was used to guarantee geometric similarity, and same construction materials, filtering and drainage media were used, so the roughness, porosity and infiltration capacity were as close as possible to the real scale, allowing a good representation of the hydraulic and treatment processes occurring in the field. The design of the synthetic and laboratory-controlled events was made based on the conditions of rainfall intensity and volume (varying the return period – RP), height of the saturated zone and underdrain head loss (Figure 2 and Table 1).

The events were designed assuring equivalence to real events in terms of rainfall in the catchment area, duration of the event, operational factors of flow rate (FR) and application rate (AR), as proposed by Macedo *et al.* (2018) for comparison

Table 1 | Description of the conditions evaluated in the synthetic events in bioretention box

Physical parameter	Condition	Description
Rainfall characteristics	Condition 1	RP = 5 years; P = 31 mm; d = 30 min; i = 62 mm/h
	Condition 2	RP = 50 years; P = 53 mm; d = 30 min; i = 106 mm/h
Saturation of filtering media	Condition a	Without saturated zone – valve height = 0 m
	Condition b	With saturated zone – valve height = 0.1 m
	Condition c	With saturated zone – valve height = 0.2 m
Underdrain head loss	Condition I	Valve completely open
	Condition II	Valve half open

RP, Return period; P, rainfall depth; d, duration; i, rainfall intensity.

of laboratory and real events (Supplementary Material – SM2). The FR represents the average velocity of the inflow and is calculated by the ratio between the average bioretention inflow of the monitored event ($\overline{Q_{\text{runoff}}}$) and bioretention surface area (A_b) (Equation (1)). The AR, conversely, represents the amortization capacity of the bioretention internal storage for a given event and is calculated by the ratio of the total runoff volume (V_{runoff}) and the total internal storage volume of the bioretention device ($V_{\text{bio,storage}}$) (Equation (2)). A list of the variables used in the equations and their description is presented in Table 2:

$$FR = \frac{\overline{Q_{\text{runoff}}}}{A_{\text{bio}}} = \frac{Q_{\text{runoff,lab}}}{A_{\text{bio,lab}}} \quad (1)$$

$$AR = \left(\frac{V_{\text{runoff}}}{V_{\text{bio,storage}}} \right) 100 = \left(\frac{V_{\text{equivalent,bio,lab}}}{V_{\text{bio,lab,storage}}} \right) 100 \quad (2)$$

In total, 26 synthetic events were monitored between January 2019 and February 2020 (Table 3). The events were performed sequentially and the antecedent dry period was varied according to periods normally found in the city of São Carlos, so that it represented the different conditions of soil saturation and biological activation usually found in the field, minimizing the effects of not comparable conditions of laboratory scale and field application (noted by Sambito *et al.* (2021) in LID studies). To assess the water quality and pollutant treatment capacity of the system, 10 events were evaluated for the parameters: chemical oxygen demand (COD), nitrogen series (nitrite – NO_2 , nitrate – NO_3 , and ammonia NH_3), phosphate – PO_4 , apparent color, pH, turbidity, total coliforms – TC, *E. coli*, metals (cadmium – Cd, chromium – Cr, copper – Cu, iron – Fe, manganese – Mn, nickel – Ni, lead – Pb and zinc – Zn), and sedimentable solids – SS. Details about the water quality dosing and sampling are provided in the Supplementary Material (SM3).

The efficiencies regarding runoff volume (Eff_{rr}), peak flow attenuation (Eff_{peak}) and time to peak attenuation (Eff_{time}) were calculated according to Equations (3)–(5). For a bioretention aiming to contribute to the SDG 6 from water recycling, the outflow is conducted to a reservoir for future non-potable reuse, and Equation (6) was used to evaluate water recovery efficiency (Eff_{wr}). In addition, the system's treatment capacity and pollutant removal efficiencies were evaluated for pollutant load ($\text{Eff}_{\text{pr,load}}$ – Equation (7)) and Event Mean Concentration (EMC) ($\text{Eff}_{\text{pr,EMC}}$ – Equation (8)). A list of the variables used in the equations and their description is presented in Table 2:

$$\text{Eff}_{\text{rr}} = \frac{V_{\text{in}} - V_{\text{over}}}{V_{\text{in}}} \quad (3)$$

$$\text{Eff}_{\text{peak}} = \frac{Q_{\text{peak,in}} - Q_{\text{peak,over}}}{Q_{\text{peak,in}}} \quad (4)$$

$$\text{Eff}_{\text{time}} = \frac{t_{\text{peak,in}} - t_{\text{peak,over}}}{t_{\text{peak,in}}} \quad (5)$$

Table 2 | List of variables

Name	Description	Dim.	Unit
<i>Rainfall equivalence – Equations (1) and (2)</i>			
A_{bio}	Surface area of a generic bioretention device	L^2	m^2
$A_{\text{bio,lab}}$	Surface area of the bioretention in laboratory	L^2	m^2
AR	Application rate	–	%
FR	Flow rate	$L t^{-1}$	m/h
Q_{runoff}	Average inflow in a generic bioretention device	$L^3 t^{-1}$	L/h
$Q_{\text{runoff,lab}}$	Runoff inflow in the bioretention in laboratory	$L^3 t^{-1}$	L/h
$V_{\text{bio,lab,storage}}$	Total storage volume of the bioretention in laboratory	L^3	L
$V_{\text{bio,storage}}$	Total storage volume of a generic bioretention device	L^3	L
$V_{\text{equivalent,bio,lab}}$	Volume equivalent to the $P_{\text{equivalent,bio,lab}}$ based on the bioretention area in laboratory	L^3	L
V_{runoff}	Total inlet runoff volume of a generic bioretention device	L^3	L
<i>Efficiencies – Equations (3)–(8)</i>			
Eff_{peak}	Peak attenuation efficiency	–	%
$\text{Eff}_{\text{pr,EMC}}$	Pollutant removal efficiency, in terms of pollutant event mean concentration	–	%
$\text{Eff}_{\text{pr,load}}$	Pollutant removal efficiency, in terms of pollutant load	–	%
Eff_{rr}	Runoff retention efficiency	–	%
Eff_{time}	Time delay efficiency	–	%
Eff_{wr}	Water reuse efficiency	–	%
EMC_{in}	Event mean concentration in the inflow	$m t^{-1}$	mg/L
EMC_{out}	Event mean concentration in the outflow	$m t^{-1}$	mg/L
M_{in}	Inflow pollutant mass	m	mg
M_{out}	Outflow pollutant mass	m	mg
$Q_{\text{peak,in}}$	Maximum inflow value	$L^3 t^{-1}$	L/h
$Q_{\text{peak,over}}$	Maximum overflow value	$L^3 t^{-1}$	L/h
$t_{\text{peak,in}}$	Duration of the event until the $Q_{\text{peak,in}}$	t	d
$t_{\text{peak,over}}$	Duration of the event until the $Q_{\text{peak,over}}$	t	d
V_{in}	Total inflow volume	L^3	L
V_{out}	Total outflow volume	L^3	L
V_{over}	Total overflow volume	L^3	L
<i>Proposed metrics to the SDG 6, 11, 13 (evaluation of water-energy-greenhouse gases nexus) – Equations (9)–(12)</i>			
CE_{cs}	Carbon emission in the conventional water supply system	m	kgCO ₂
CE_{hs}	Carbon emission in the hybrid system	m	kgCO ₂
CER_{hs}	Carbon Emission Reduction of hybrid systems	$m L^{-4}$	$10^{-6} \text{ kgCO}_2/\text{m}^2 A_{\text{bio}}/\text{m}^2 I A_c$
ED_{cs}	Energy demand in the conventional water supply system	E	kWh
ED_{hs}	Energy demand in the hybrid system	E	kWh
EDR_{hs}	Energy Demand Reduction in hybrid systems	$E L^{-4}$	$10^{-6} \text{ kWh}/\text{m}^2 A_{\text{bio}}/\text{m}^2 I A_c$
$I A_c$	Impervious catchment area	L^2	m^2
$V_{\text{out,rec}}$	Recovered outflow volume available to non-potable reuse	L^3	m^3
WD	Total water demand from the centralized water supply system	L^3	m^3
WDR_{hs}	Water Demand Reduction in hybrid systems	L^{-1}	$10^{-6} \text{ m}^3/\text{m}^2 A_{\text{bio}}/\text{m}^2 I A_c$
WSR	Water Stress Reduction index	–	%

Table 3 | Description of the synthetic events, operation factors and water balance

Event	Date	Type	FR (m/h)	AR (%)	d (min)	API (mm)	Dry days	Quality monitoring	V _{in} (L)	V _{out} (L)	V _{over} (L)	V _{storage} (L)	Q _{in} (L/h)	Q _{peak,out} (L/h)	Q _{peak,over} (L/h)	Group EMC	Group Load
1	1/29/2019	1.a.I	1.0	239	29.0	–	–	No	701.32	618.15	0	83.17	1,451	1,320	0	–	–
2	1/30/2019	1.a.II	1.0	240.0	29.2	31.0	0	No	705.35	656.85	0	48.5	1,451	822	0	–	–
3	1/31/2019	1.b.I	1.0	243.0	29.6	46.5	0	No	714.62	549.78	0	164.84	1,451	864	0	–	–
4	2/1/2019	1.b.II	1.0	239.0	29.0	56.8	0	No	701.32	590.7	0	110.62	1,451	736	0	–	–
5	2/4/2019	1.c.I	1.0	251.0	30.4	29.5	2	No	735.95	633.55	0	102.4	1,451	792	0	–	–
6	2/6/2019	1.c.II	1.0	249.0	30.3	35.2	1	No	731.95	667.7	0	64.25	1,451	680	0	–	–
7	3/11/2019	2.a.I	1.6	405.0	31.4	5.0	32	No	1187	975.6	6	205.4	2,268	1,128	72	–	–
8	3/12/2019	2.a.II	1.6	392.0	30.4	57.8	0	No	1,150.38	865.1	121.3	163.98	2,268	852	924	–	–
9	3/13/2019	2.b.I	1.6	440.0	34.2	84.2	0	No	1,290.87	985.8	159	146.07	2,268	1,110	930	–	–
10	3/14/2019	2.b.II	1.6	391.0	30.4	101.8	0	No	1,147.86	881.4	147	119.46	2,268	816	1,092	–	–
11	3/19/2019	2.c.I	1.6	396.0	30.8	37.7	4	No	1,162.98	860	177.8	125.18	2,268	864	1,188	–	–
12	3/28/2019	2.c.II	1.6	412.0	32.0	23.0	8	No	1,209.6	881.2	191.7	136.7	2,268	924	1,206	–	–
13	5/27/2019	1.a.I	1.0	246.0	30.0	6.1	59	Yes	721.44	592.55	0	128.89	1,442.89	840	0	0	0
14	6/10/2019	1.a.II	1.0	249.0	30.4	7.4	13	Yes	731.03	655.65	0	75.41	1,442.89	666	0	0	0
15	6/26/2019	1.c.I	1.0	255.0	31.1	7.4	15	Yes	747.9	520.7	0	227.2	1,442.89	498	0	0	0
16	8/6/2019	1.c.II	0.7	170.0	28.8	5.0	40	Yes	500	392.2	0	107.8	1,040.46	456	0	1	1
17	8/19/2019	1.a.I	1.0	238.0	30.2	6.8	12	Yes	697.31	456.5	0	240.81	1,384.62	744	0	0	0
a1	8/20/2019	a.I	1.0	87.0	10.6	37.5	0	No	473.08	455.3	0	17.78	1,384.6	564	0	–	–
a2	8/20/2019	a.II	1.0	82.0	10.1	48.5	0	No	692.31	582	0	110.31	1,384.6	648	0	–	–
a3	8/21/2019	c.I	1.0	82.0	10.0	43.9	0	No	255.71	224.3	0	31.41	1,442.89	536	0	–	–
a4	8/21/2019	c.II	1.0	82.0	10.0	54.9	0	No	242.89	234	0	8.89	1,442.89	585	0	–	–
18	9/2/2019	1.c.I	1.0	161.0	20.5	10.8	11	Yes	240.48	214	0	26.48	1,442.89	336	0	0	1
19	9/30/2019	1.c.I	1.0	236.0	30.0	6.7	27	Yes	240.48	265.2	0	–24.72	1,442.89	348	0	0	0
20	1/21/2020	1.c.I	1.0	232.0	29.5	3.1	112	Yes – N series	680.77	550.7	0	130.07	1,384.62	588	0	–	–
21	1/28/2020	1.c.I	0.9	236.0	30.0	7.5	6	Yes – N series	692.31	642.5	0	49.81	1,348.6	618	0	–	–
22	2/11/2020	1.c.I	0.9	236.0	30.0	6.5	13	Yes – N series	692.3	656	0	36.3	1,348.6	666	0	–	–

FR, Flow rate; AR, Application rate; d, Duration; API, Antecedent precipitation index; Dry days, days with 0 mm of precipitation; V_{storage}, final stored volume; Q_{in}, inflow; Q_{peak,out}, outflow peak.

$$\text{Eff}_{\text{wr}} = \frac{V_{\text{out}}}{V_{\text{in}}} \quad (6)$$

$$\text{Eff}_{\text{pr,load}} = \frac{M_{\text{in}} - M_{\text{out}}}{M_{\text{in}}} \quad (7)$$

$$\text{Eff}_{\text{pr,EMC}} = \frac{\text{EMC}_{\text{in}} - \text{EMC}_{\text{out}}}{\text{EMC}_{\text{in}}} \quad (8)$$

2.1.2. Statistical design

The statistical evaluation was made in two stages: (1) Exploratory Data Analysis (EDA) and (2) clustering evaluation of the efficiencies. Statistical analysis was performed using the Python library SciPy 1.5.0 (PyPi 2020a; Virtanen *et al.* 2020), scikit-posthocs 0.6.1 (PyPi 2019) and scikit-learn 0.23.2 (Pedregosa *et al.* 2011; PyPi 2020b).

For the EDA, the data were grouped in three different ways: (1) regarding water balance variables and their efficiencies; (2) regarding pollutant removal; and (3) regarding the bioretention configuration for saturation and head loss. For the EDA, descriptive statistical measures of the results and hypothesis tests for comparison of runoff retention, water reuse, and pollutant removal efficiency medians for independent groups, using the non-parametric Kruskal-Wallis test and Dunn's test were performed. All statistical tests were evaluated for significance level $\alpha = 0.10$ (Helsel *et al.* 2020).

The clustering aimed to identify patterns and operational key-factors in the groups according to the efficiencies of runoff retention, water reuse and pollutant removal. The Hierarchical Agglomerative Clustering (HAC) method was used. After the construction of the dendrogram, the groups were separated according to the Elbow method.

2.2. Contribution of hybrid systems of water supply and urban drainage to SDGs in watershed scale

The use of bioretention devices with stormwater harvesting can integrate the approach of hybrid water supply and drainage systems (Sapkota *et al.* 2015). The hybrid systems allow a reduction in energy demands, increasing the integrated resilience of water and energy systems. Consequently, from the approach of the *water-energy-greenhouse gas nexus* (Nair *et al.* 2014), the reductions in energy demand in hybrid systems also contribute to the reduction of GHG emissions (Arora *et al.* 2015). From this holistic perspective, the hybrid systems integrated with LID evaluated in this study can also contribute to SDG 6, SDG 11 and SDG 13, since they reduce water stress and diversification of water sources, reduce the energy demands and carbon emissions by adopting decentralized systems, and increase the catchment resilience to floods and droughts, reducing the directly affected persons due to disasters.

In this study, we evaluate the contribution of the bioretention systems to the *water-energy-greenhouse gas nexus* using the metrics presented in Equations (9)–(12), at the Mineirinho watershed (Figure 3).

Equation (9) presents the reduction in tap water demands from central supply systems due to the recovery of water for non-potable use in bioretention systems, at individual level (per household). This indicator is called water stress reduction index (WSR) and is calculated in absolute terms, proportional to the total water demand from central systems (final values ranging from 0 to 1). Conversely, Equation (10) presents a generalization of the indicator presented in Equation (9) for the entire catchment, and it is called water demand reduction in hybrid systems (WDR), however, the reduction in tap water demand from the central system is calculated in proportion to the sum of bioretention area in the catchment ($\sum A_b$) and the total impervious area of the catchment (IA_c). Indicators were also built for Energy Demand Reduction (EDR – Equation (11)) and Carbon Emission Reduction (CER – Equation (12)) in the catchment, in which the difference between energy demands and carbon emission of a central system (ED_{cs} and CE_{cs}) and a hybrid system (ED_{hs} and CE_{hs}) for water supply and stormwater management are calculated, and proportional to $\sum A_b$ and IA_c . A list of the variables used and their description is presented in Table 2:

$$\text{WSR} = 1 - \left(\frac{\text{WD} - V_{\text{out,rec}}}{\text{WD}} \right) \quad (9)$$

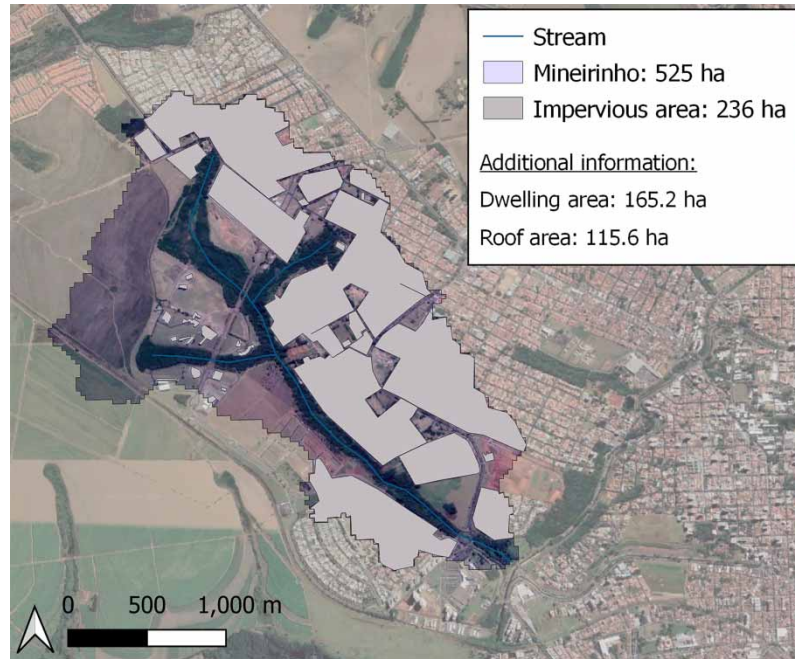


Figure 3 | Mineirinho watershed area and occupation characteristics.

$$WDR_{hs} = 1 - \frac{\sum (WD - V_{out,rec}) / \sum A_b}{IA_c} \quad (10)$$

$$EDR_{hs} = \frac{ED_{cs} - ED_{hs} / \sum A_b}{IA_c} \quad (11)$$

$$CER_{hs} = \frac{CE_{cs} - CE_{hs} / \sum A_b}{IA_c} \quad (12)$$

The reduction in the water demand in households was quantified according to the sequential steps to quantify average household demand, average water volume stored in individual bioretention systems and average monthly rainfall, presented in the Supplementary Material (SM4). After the evaluation for one household, an optimistic scenario of the use of bioretention structures coupled to reservoirs for water reuse in all residences in the Mineirinho watershed was raised. The total number of residences in the watershed was estimated using image classification in QGIS 3.12 software (Figure 3) (Supplementary Material – SM5). Finally, the water demand for non-potable use and the water recovery from the bioretention for the watershed were obtained from the extrapolation of data from one household to the total number of residences allocated in the watershed. Then, it was possible to obtain a total reduction in water demands from the central supply system in the entire watershed area.

To quantify the energy demands and carbon emissions for the central and hybrid systems, we obtained: (1) the average energy demand of the water supply networks for the city of São Carlos for the year of 2018 (SNIS 2018): 1.2 kWh/m³, and (2) the average monthly CO₂ emission value per unit of energy produced by the National Interconnected System (MCTIC 2020).

It is important to remark that this methodology aims at an approximate estimation of the reduction in water demand and stress, in energy demand and in carbon emission, and to provide an initial assessment of the contributions and benefits of using hybrid systems to catchment scale. Most accurate estimations should account with multi-story buildings from residential registration at city hall, modeling of individual bioretention systems to each household, and continuous modeling with typical rainfall year. Due to lack of good quality data to provide this more detailed and comprehensive analysis, in this study we chose to provide an initial assessment with approximate indicators values representing the contribution to the *water-energy-greenhouse gases nexus* and SDG 6, 11 and 13.

3. RESULTS AND DISCUSSION

3.1. Description of monitored events and exploratory analysis

3.1.1. Runoff quantity results

Table 3 presents the 26 monitored events and their descriptions in terms of the operational factors, previous drought conditions and water balance. The monitored events cover a wide range of previous drought condition variability, ranging from events with less than one dry day, to up to 4 months of drought (condition that occurs in the city of São Carlos, during dry winters). In addition, four events with a shorter duration (10 min) were monitored as a chain of events, classified as a1, a2, a3 and a4.

Figure 4 presents the average hydrographs and their confidence intervals for each configuration evaluated, according to the event intensity. For events with greater recurrence (RP = 5 years and $d = 30$ min, condition 1), no overflow was observed for any of the configurations. The increased head loss in the underdrain (condition II) and the presence of a saturated zone (conditions b and c) did not affect the runoff retention efficiency, while they presented greater outflow amortization. If there is no water recovery for reuse, a more amortized outflow contributes to the reduction of flood events.

However, for more extreme events (RP = 50 years and $d = 30$ min, condition 2), the presence of a saturated zone and greater head loss led to a greater overflow and a slight reduction in outflow. For condition II, this behavior can be explained by the restriction of the maximum flow in the underdrain due to the insertion of the head loss, limiting the infiltration into the filtering media and increasing ponding depth. In the case of conditions b and c, the presence of the saturated zone reduces the initial useful storage volume in the filtering media. Conditions b and c, however, were not much affected by the insertion of additional head loss in the underdrain.

Figure 5(a) shows boxplots for the water balance variables and different configurations. When comparing the head loss conditions, configuration II resulted in greater overflow, less outflow and less storage. For different saturation, there was an increase in storage when comparing configurations a and b, while it was kept constant when comparing configurations a and c. The storage in the water balance in Figure 5(a) considered the water stored in the filtering media and in the ponding zone, therefore, as almost all flow was retained for Type 1 events, there was no big difference in total storage. Type b events had higher storage values because they also had a higher median inflow value.

Figure 5(b) presents the boxplots for runoff retention, peak attenuation and water reuse efficiencies, as a more uniform scale measure for the different configurations. The Kruskal–Wallis test for runoff retention efficiency (statistics = 2.313 and p -value = 0.804), water reuse efficiency (statistics = 3.715 and p -value = 0.591) and peak flow attenuation (statistics = 2.215 and p -value = 0.819) failed to reject the null hypothesis, concluding that there is no difference in their medians for the different configurations.

This result seems contradictory when comparing with the discussions for the hydrographs in Figure 4. However, as shown in Table 3, Type 2 events (RP = 50 years) were carried out in lower numbers when compared to Type 1 events, especially for configurations a and c, and were considered outliers in the boxplot (Figure 5(b)). Since the median is a central value measurement that is more resistant to outliers (Helsel *et al.* 2020), Type 1 events had greater influence on the distribution and central value and, therefore, the Kruskal–Wallis test failed to reject the null hypothesis. Therefore, we recommend future evaluations incorporating more extreme events, which allow performance of a test of central values in more representative distributions, to assess whether in fact the adoption of a saturated zone leads to large losses in peak flow attenuation efficiency.

It is also important to carry out further studies evaluating a greater amount of chain of events and for longer durations, since in this study only two series of chain events were monitored (a1 and a2, a3 and a4) with reduced duration ($d = 10$ min). Macedo *et al.* (2019a) have noted significant reduction in the runoff retention and peak flow attenuation efficiencies of an experimental bioretention system in field due to chain events. Soil saturation and/or water storage in the ponding zone from previous events not yet completely emptied can lead to significant drops in the efficiency of runoff retention and peak flow attenuation, compromising the runoff and flood control function of the system. Similar conclusions were obtained in the study of Freni & Liuzzo (2019) on rainwater harvesting systems aimed at runoff control through continuous modeling, noting that the efficiency of the system from a single event and the average efficiency in the long period may differ significantly.

3.1.2. Water quality results

The improvement of water quality by the adoption of bioretention practices was also assessed. For this purpose, 10 events were evaluated, for configurations a and c, as they presented the greater difference regarding water balance variables. A

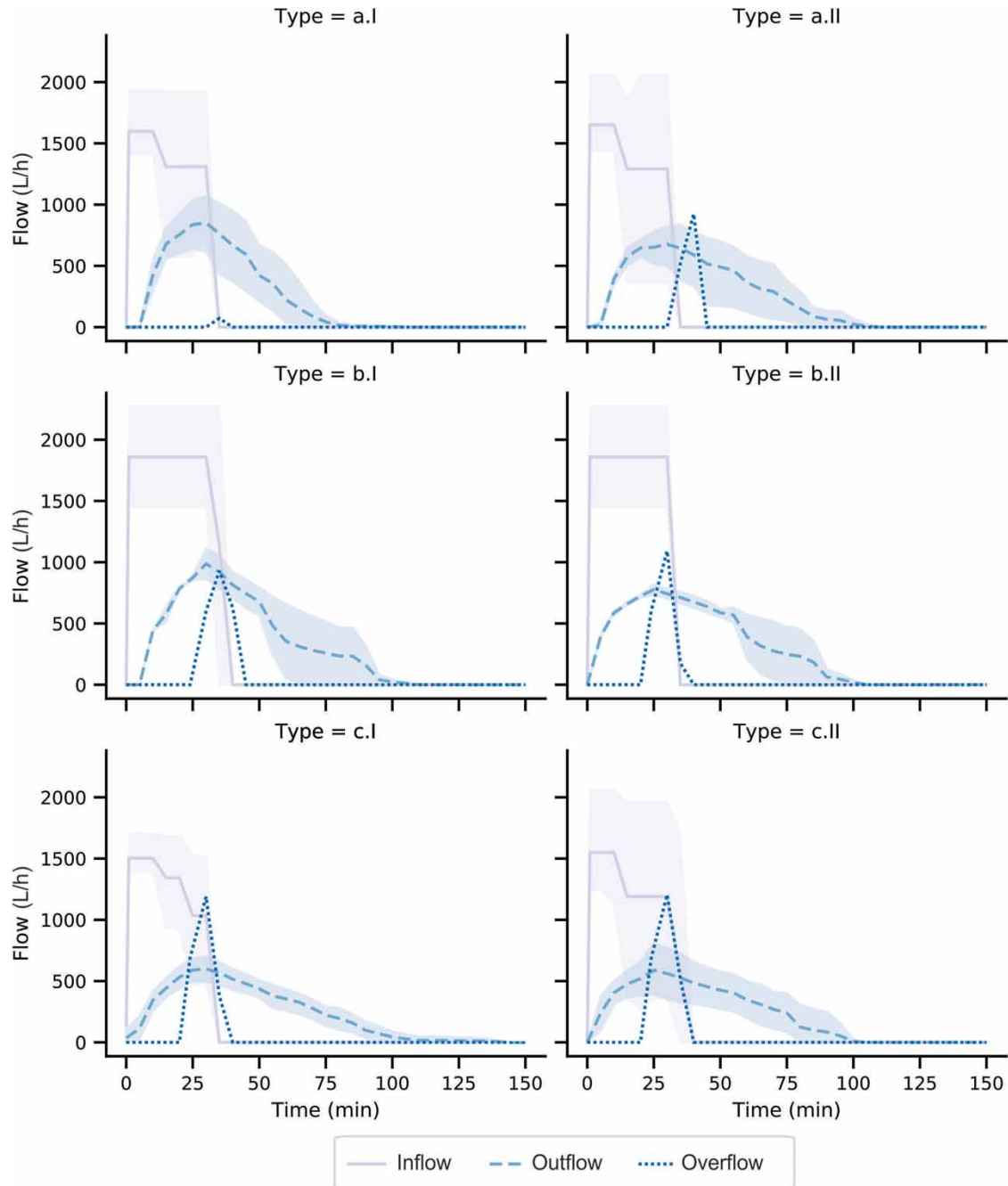


Figure 4 | Hydrographs grouped by different configurations in terms of saturated zone and underdrain head loss. Differences in inflow for Types 'a' and 'c' were due to events with different duration.

previous evaluation for all configurations did not show any difference in the water quality from different head losses. Therefore, the experiments continued to be conducted only with condition I, as it was more efficient when assessing the water balance.

The average concentration pollutographs with their confidence intervals obtained for configurations a and c can be seen in Figure 6. For Cr, Cu, Pb, Mn, Ni, Cd the samples had concentrations lower than the detection limits; thus, pollutographs were not constructed for these pollutants. In general, for configuration a (Figure 6 - Type = a) almost all pollutants had peak values for outflow concentration higher than the inflow. Exceptions can be noted for COD, PO₄, NO₂, Zn and TC for their average

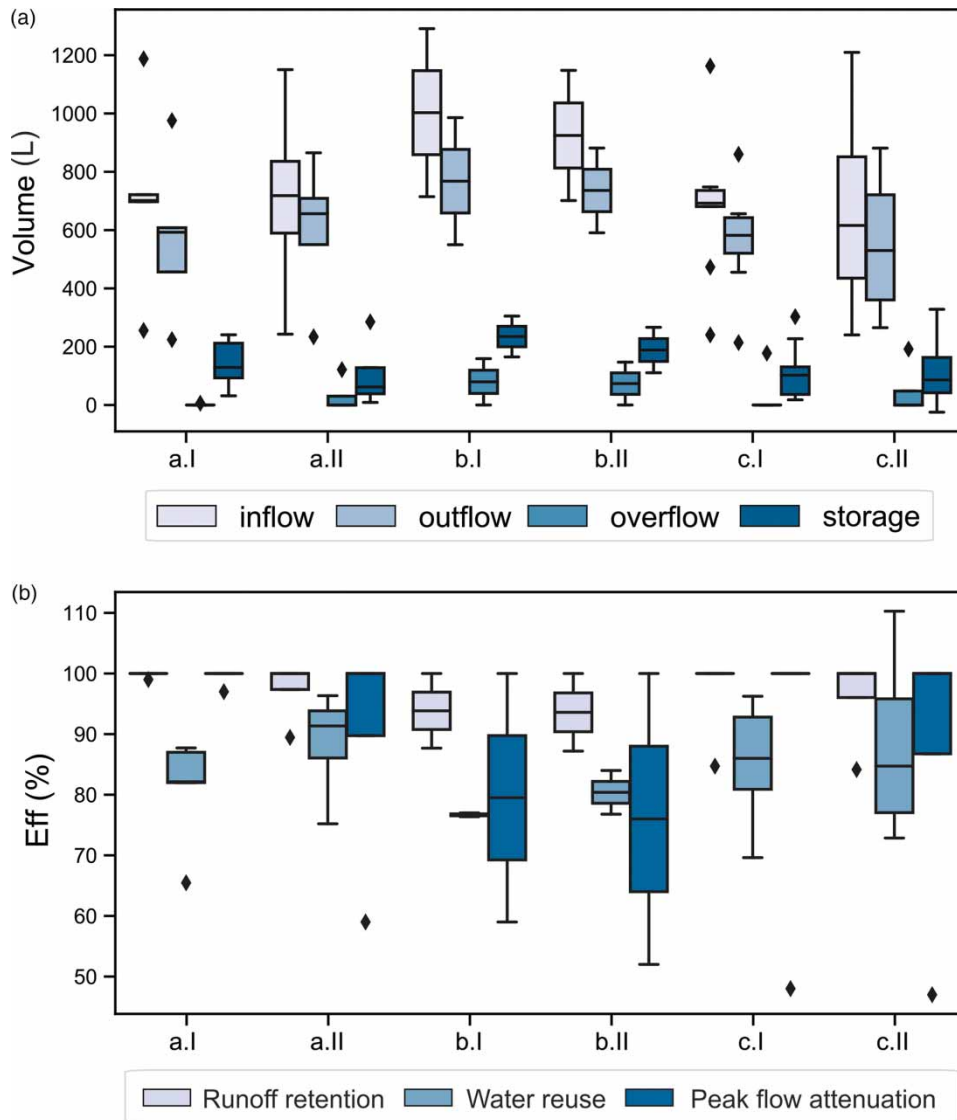


Figure 5 | Boxplot for different configurations considering: (a) water balance variables and (b) efficiencies of runoff retention, water reuse and peak flow attenuation.

values, however, the upper confidence interval sometimes exceeded or equaled the inflow concentrations. NO_3 , NH_4 , Fe and *E. coli* presented the greatest export, in addition to the turbidity and color that are not measured in concentration.

For the nitrogen series, several studies have obtained the export of total nitrogen or its fractions in bioretention systems without a saturated zone (Davis *et al.* 2006; Payne *et al.* 2014a; Mangangka *et al.* 2015; Chahal *et al.* 2016). The export of this nutrient in vegetated systems occurs mainly due to two processes, which prevails depending on the filtering media characteristics and the system configuration: (1) the first hypothesis is due to the initial composition of the filtering media and presence of plants. There may be initial amounts of high nutrients or release of nitrogen due to the death of the plants, which leach from the soil along with the water movement (Payne *et al.* 2014b). Because nitrogen is more mobile than phosphorus (mainly the NO_3 fractions when compared to PO_4), due to its higher solubility, low adsorption and low sedimentation, the leaching process is more marked for this nutrient (Roy-Poirier *et al.* 2010; Laurenson *et al.* 2013); (2) The second hypothesis is due to the natural processes of the nitrogen cycle that occur intra-events. During periods of drought and in the presence of aerobic environments, there is the transformation of NH_4 into NO_2 and later NO_3 , which accumulates in the water and are later released. The presence of a saturated zone can assist in the denitrification process, converting the residual NO_3 into nitrogen gas, removing it permanently from the system (Payne *et al.* 2014a, 2014b).

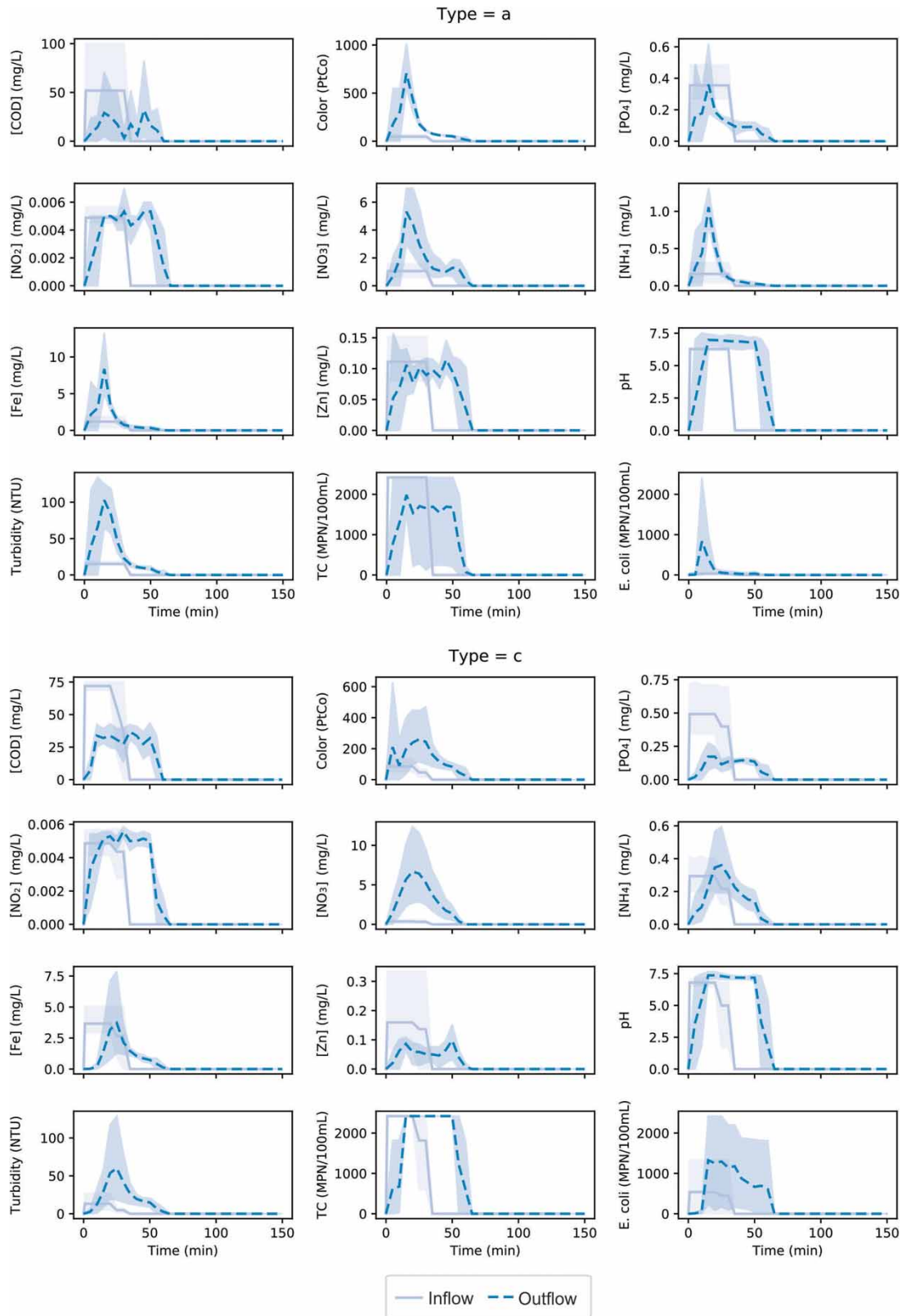


Figure 6 | Concentration pollutographs for different water quality parameters and different configurations.

The export of iron can be explained by the composition of the filtering media. The natural soil of São Carlos region is predominantly of the Type Red-Yellow Oxisoil (Macedo *et al.* 2019a), presenting large amounts of ferrous oxide goethite (FeO) and hematite (Fe₂O₃), and clay texture. Evaluating the results of color and turbidity together, we can notice an increase in these two parameters in the outflow when compared to the inflow, indicating a greater amount of dissolved and suspended solids in the output of the systems. However, in the SS evaluation, for all events and configurations, the value of this parameter in the outflow was null, showing that the solid particles in the outflow are colloidal, a characteristic of soils with a clay texture. We can conclude that the export of iron in these systems is due to the transport of soil particles along with the outflow. Similar results were observed by Macedo *et al.* (2019a), in the evaluation of bioretention applied in the field. They noticed export of Fe in the overflow mainly in the occurrence of erosion of the top vegetated layer also composed of Red-Yellow Oxisoil.

Regarding *E. coli* the increased presence of this microorganism in the outflow may be related to (a) desorption after long drought events (Shen *et al.* 2018); and (b) external contamination during the sampling process, or proliferation between collection and analysis. Learning from this study to avoid contamination and proliferation of *E. coli*, we suggest that further experiments should be conducted in complete closed environments (avoiding the presence of animals), cleaning gloves and analysis material with alcohol 96 °GL, cleaning collection materials between samples and between events with chlorine or alcohol 96 °GL (when possible), and making different people responsible for sampling inlet and outlet, and event registration.

For configuration c (Figure 6 – Type = c) a general improvement for all pollutants is noticeable. For COD, and PO₄, the average values and upper limits for outflow concentration no longer exceed the inflow concentrations, and for Fe the average outflow value also decreases when compared to the inflow, having less export than configuration a. The color and turbidity values are also lower when compared to configuration a, although they are still higher than the outflow. This improvement can be explained by the presence of the saturated zone providing a longer retention time for a portion of water retained between events, favoring the occurrence of physical–chemical–biological processes.

This water retention process between events is also explained by Shen *et al.* (2018), presenting this differentiation based on the terms ‘old water’ – the portion retained from the previous event due to the presence of the saturated zone, and ‘new water’ – the portion of the outflow that corresponds only to the current monitored event. In ‘old water’ the processes of sedimentation, adsorption and biological degradation are more significant, due to longer settling time, longer contact time between particle-filtering media and particle-biofilm, and higher plant uptake and evapotranspiration fluxes of the water/pollutant mixture. This process can be visually noticed when comparing samples with and without saturated zone, for apparent color (Figure 7). It is possible to observe the further displacement of solid peaks for configuration c, which corresponds to the water volume retained in the saturated zone at the beginning of the event.

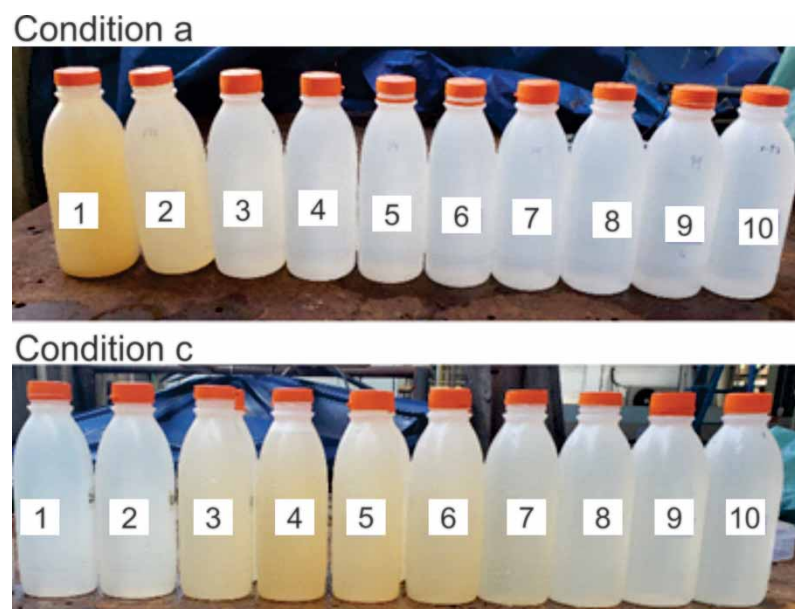


Figure 7 | Apparent color over samples collected at 5 min intervals for ‘configuration a’ and ‘configuration c’.

The inclusion of the saturated zone is indicated mainly to assist in the removal of NO_3 , due to the creation of an anaerobic zone allowing the occurrence of the denitrification process. For this study, we observed that the presence of the saturated zone helped to reduce NH_4 , the longer detention time favored the nitrification reactions and/or plant uptake. However, it was not possible to observe an improvement in the treatment of NO_3 for configuration c, and even an increase in its export was observed. Two hypotheses can explain this behavior: (1) the export of NO_3 occurs mainly due to the presence of a large amount of nitrogen fractions in the filtering media and the leaching rates exceeds the denitrification rates; (2) denitrification occurs at low rates due to a lack of sufficient dissolved carbon to serve as an energy source for denitrifying bacteria. From Figure 6, low amounts of DOC in the outflow for both configurations can be seen, and even smaller for configuration c. An internal carbon source was not used in this study, which is usually indicated to assist in denitrification (Kim *et al.* 2003; Payne *et al.* 2014b), to assess the possible contribution of denitrification in removing organic matter in the runoff and acting as a pathway to carbon sequestration.

We also observed an average increase in the concentrations of TC and *E. coli*, for configuration c. Stott *et al.* (2017) noted less microbial retention in systems with saturated zones. Conversely, Søberg *et al.* (2019) found a reduction in the concentration of bacteria in the saturated zone; however, the increase in temperatures also increased the outflow concentrations. For this study, there was no conclusion due to the possibility of sample contamination.

In addition to assessments of concentration-based pollutant removal, assessments for load are also recommended, since the effect of reducing volumes also contributes to reducing the pollution, which is not verified by concentration-based analysis (WWEGC 2007; Jones *et al.* 2008; Lago *et al.* 2017). Therefore, Figure 8 also presents the load pollutographs. Comparing the inflow load values with the outflow, almost all pollutants present a significant reduction in the pollutant peaks, except for NO_3 , NH_4 and Fe for configuration a, and only for NO_3 in configuration c.

To assist in the interpretation of the results regarding the differences brought by the adoption of the two different configurations in the pollutant removal efficiencies, in Figure 9 are presented boxplots of the efficiencies for EMC and load. For some of these parameters, their typical values are low, e.g. NO_2 and metals (with the exception of Fe), therefore, there may be uncertainties and biases related to the measurement methods.

The efficiencies for configuration c are in general greater than that for configuration a, except for NO_3 , *E. coli* and TC, as already observed by the pollutographs. The Kruskal–Wallis test resulted in no difference for EMC and load for almost all parameters. Exception was noted to NO_3 and NH_4 (statistics = 2.92 and p -value = 0.087) for nutrients, and Fe (statistics = 3.86 and p -value = 0.05) for metals, obtaining better efficiencies in configuration a for NO_3 and in configuration c for NH_4 and Fe.

However, the lower efficiency for NO_3 in configuration a does not necessarily indicate less removal capacity caused by the presence of the saturated zone, but rather a greater conversion of NH_4 to NO_3 (since the efficiency of NH_4 removal was increased). Therefore, the two configurations are equally inefficient in removing this pollutant.

3.2. Identification of clusters and their characteristics

A clustering analysis of the events was performed regarding the runoff retention and water reuse efficiencies (Eff_{rr} and Eff_{wr}), EMC-based and load-based pollutant removal efficiency ($\text{Eff}_{\text{pr,EMC}}$ and $\text{Eff}_{\text{pr,load}}$). The clustering analysis aimed to identify operational key-factors or hydro-meteorological patterns that determine similar water balance and water quality behaviors.

Regarding the clusters on water balance, three main groups were identified (Figure 10): Group 0 = [Event 1, 2, 5, 6, 14, 18, 21, 22, a1, a2, a3, a4]; Group 1 = [Event 3, 4, 7, 13, 15, 16, 17, 19, 20] and; Group 2 = [Event 8, 9, 10, 11, 12]. Three different hydro-meteorological patterns were identified when the characteristics of the events were evaluated (Table 3). Group 0 is formed by recurrent events (5 years RP), with little dry period between them, ranging from 0 to 13 days, and APIs ranging from 6.5 to 54.9 mm, but with a greater predominance of values above 29 mm. This pattern resulted in events with intermediate outflow and Eff_{wr} values. Group 2 also has a well-defined pattern, characterized by extreme events (50 years RP), with a short dry period between them (<8 days) and high APIs, ranging from 23 to 101.8 mm. This pattern resulted in overflow and high outflow values. Finally, Group 1 has more distinct characteristics between the events. In general, the observed pattern is of events with 5 years RP, i.e. more recurrent, with large periods of previous drought, ranging from 12 to 59 days and with low API values, ranging from 3.1 to 5.0 mm. Some exceptions are observed: events 3 and 4 have high API (46.5 and 56.8 mm, respectively) and zero previous drought days. These two events are Type b, so the presence of a saturated zone and the weather conditions of the day must have led to smaller outflows and higher Eff_{rr} and Eff_{wr} . In addition, event 7 is also an exception, as it is an event with 50 years RP, however, this event occurred after a long drought period (112 days) with low

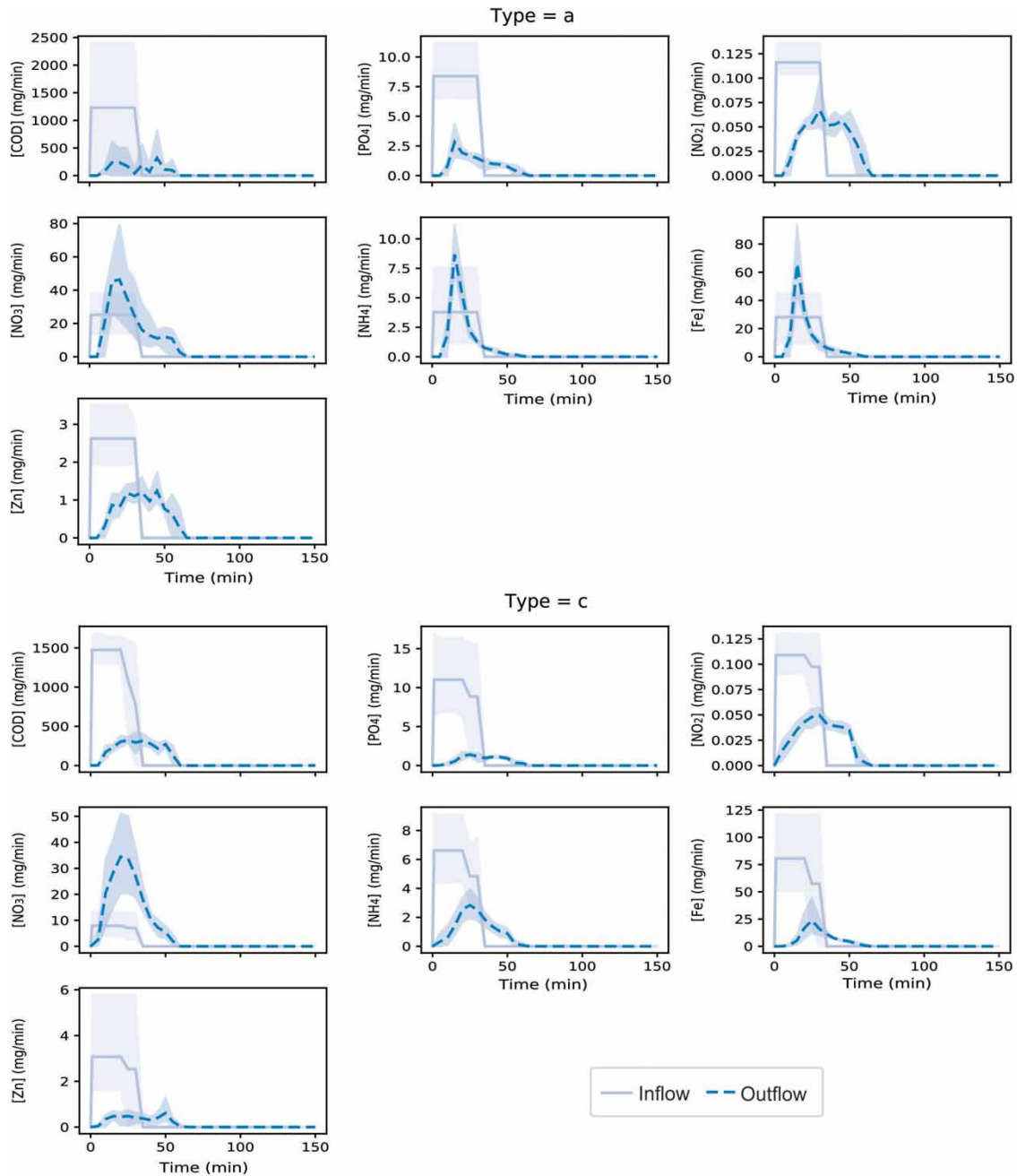


Figure 8 | Load pollutographs for different water quality parameters and different configurations.

API (3.1 mm), leading to practically no formation of overflow and great water retention in the pores, resulting in low outflow (behavior that can be noticed in Figure 4 for Type a.I event).

As for $Eff_{pr,EMC}$, two main groups were identified (Figure 10): Group 0 = [Event 13, 14, 15, 17, 18, 19] and Group 1 = [Event 16]. For event 16, there is a high nitrogen export, a behavior that differs significantly from other events. The other variables describing the events (Table 3) do not present clear distinct patterns to characterize different clusters. Therefore, the high nitrogen export on event 16 is due to operation factors (FR and AR), instead of its hydro-meteorological characteristics.

Finally, regarding $Eff_{pr,load}$, two groups were identified (Figure 10): Group 0 = [Event 13,14, 15, 17, 19] and Group 1 = [Event 16, 18]. The two groups have similar characteristics of drought periods and API, ranging from 12 to 59 dry days and API of 6.1 to 7.4 mm for Group 0, and 11 to 40 dry days and API of 5.0 to 10.8 mm for Group 1. Additionally,

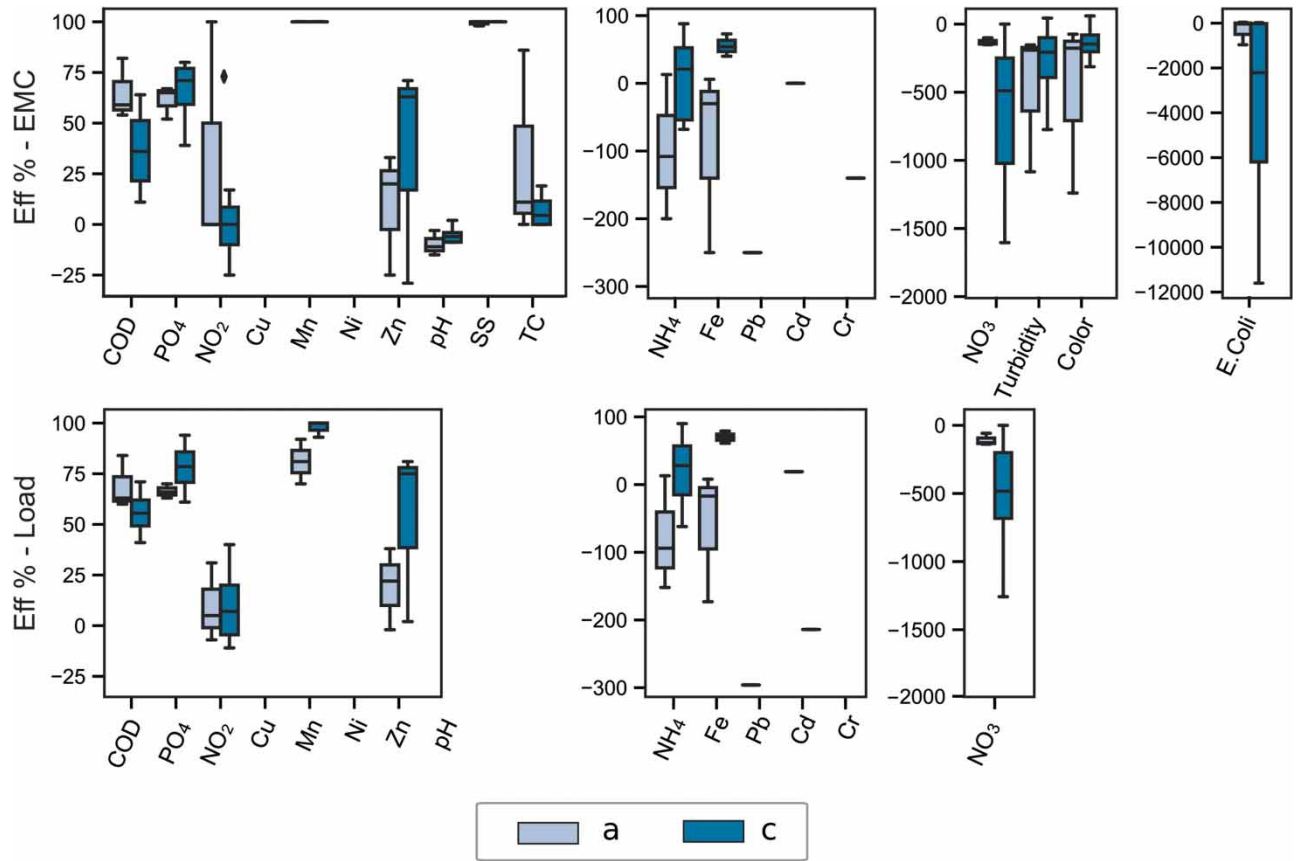


Figure 9 | Boxplot for pollutant removal efficiencies by configurations and by evaluation variable (EMC or load).

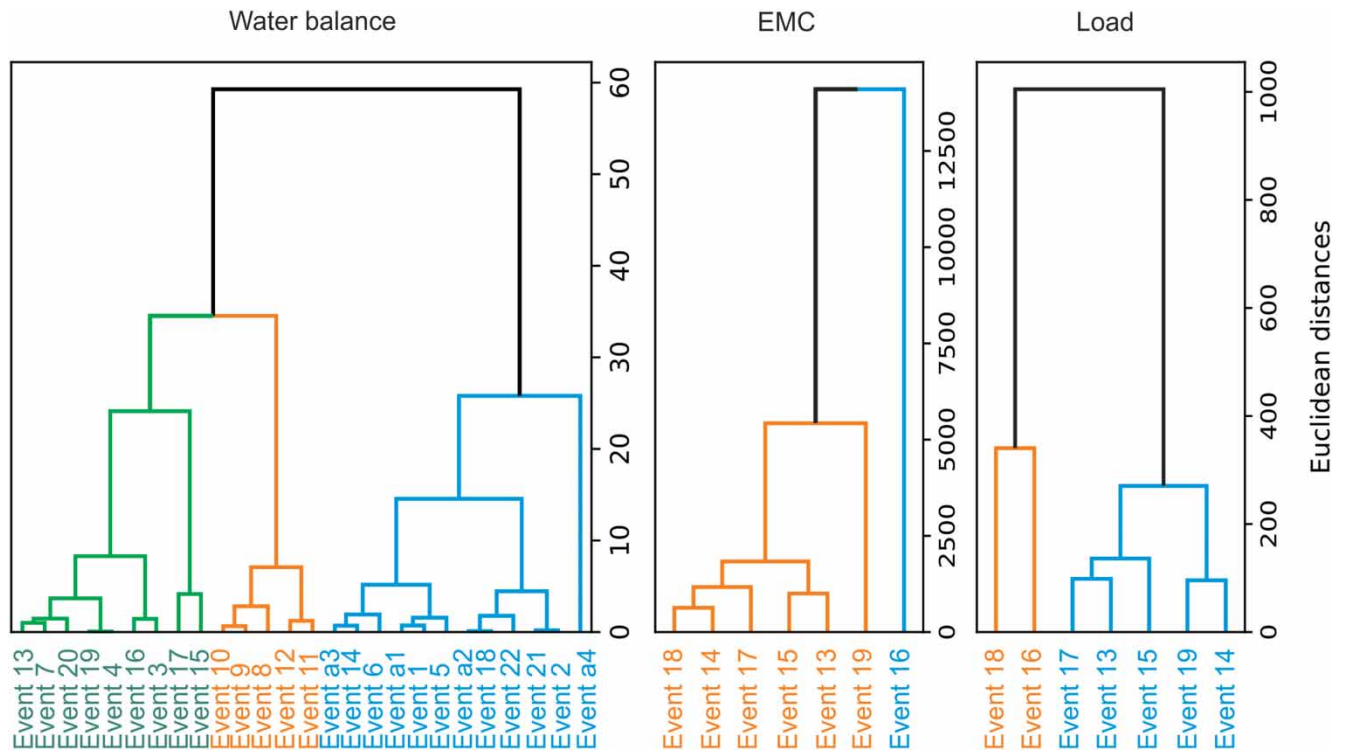


Figure 10 | Dendrogram of the HAC, highlighting the different clusters identified.

both groups have rainfall equivalent to 5 years RP. The main differentiation between the two groups occurs in terms of AR, so that Group 1 has applied volumes of 161 and 170% of the total volume available in the technique, while group 0 has AR ranging from 236 to 255%. Smaller AR leads to smaller outflows, and consequently lower pollutant loads due to volume retention (WWEGC 2007; Jones *et al.* 2008). In addition, both events are Type c, which has been shown previously to have slightly lower loads over time, and higher efficiencies than Type a (Figures 6, 8 and 9).

The Kruskal–Wallis test did not show differences in the Eff_{rr} values regarding the different bioretention configurations (with and without the saturated zone). Accordingly, it was not possible to notice the influence of the configurations in the cluster formation, for water balance. The hydro-meteorological characteristics of the events could explain different behavior patterns, which were also observed and analyzed in Macedo *et al.* (2019b), demonstrating the correlation between dry days and API with Eff_{rr} . It is important to point out that the small number of extreme events monitored in this study may have resulted in loss of information on the influence of the different configurations on Eff_{rr} and, consequently, on water balance clustering.

Regarding $Eff_{pr,EMC}$ and $Eff_{pr,load}$, the Kruskal–Wallis test showed a difference between the configurations for NO_3 , NH_4 and Fe pollutants. In the cluster analysis, the efficiencies for all pollutants are assessed in an integrated manner. Therefore, the configuration of each event was not decisive in the formation of the groups. The event characteristic with the greatest influence for the cluster formations for water quality was the AR, which represents a measure of the event magnitude regarding the bioretention useful volume.

3.3. Contribution to SDGs from the water-energy-greenhouse gas nexus

In this section, we intended to carry out an initial quantification of how bioretention structures aiming at both runoff control (quantity and quality) and water reuse can contribute to the SDGs and provide improvement in watershed management. Therefore, the reductions in water demand at residential and watershed scale, and reductions in energy demands and carbon emissions at watershed scale were raised.

Two types of possible reuse for households were raised, relying on water demands for washing machines, external usage and sanitary discharge – non-potable demand (NPD) Type 1, and only external use and sanitary discharge – NPD Type 2. For the NPD-Type 1, a demand of $6.3 \text{ m}^3/\text{month}$ was obtained, and for NPD-Type 2, a demand of $2.8 \text{ m}^3/\text{month}$ was obtained.

The monthly demand was contrasted with the volume of recovery water by the bioretention, identifying the months in which NPD-Type 1 and Type 2 are completely supplied and how this translates into the water stress reduction (WSR) indicator proposed in this study (Table 4). For the city of São Carlos, there is a strong variation between total rainfall volume in the wetter and drier months, as well as dry days, reaching average values of up to 28 days without rain in the driest month. This pattern in rainfall and dry periods also leads to a great difference in the recovered water volume. For January, up to 23.4 m^3 of water can be recovered, significantly exceeding non-potable demands, for both Type 1 and Type 2. However, the reuse reservoir has a capacity of 1 m^3 , preventing the storage of the entire recovered volume for future dry months. The excess of recovered water per event returns to the watershed through infiltration to groundwater or as runoff to the drainage system or directly to the stream.

For May to September there was a deficit in the total recovered water volume for NPD-Type 1, and in July and August for NPD-Type 2, i.e., the amount of water recovered is not sufficient to meet these demands. An alternative would be to install additional reservoir modules. With the adoption of one more module it would be possible to supply the NPD-Type2 for the entire year. For NPD-Type1, 15 more modules would be needed, which is impractical due to space and cost. However, there is already a 45% saving for 7 months of the year with reuses for Type 1, which contribute to the general security of the water supply system.

Monetary savings per household due to stormwater harvesting were also raised. For the city of São Carlos, the taxes currently practiced by the water supply company are $6.3 \text{ R\$/m}^3$ (equivalent to US\$ 1.2 for the year 2020), for demand ranges from 11 to 15 m^3 (ARES-PCJ 2019). Therefore, the water reuse from bioretention systems can lead to savings of up to R\$ 385/household/year (US\$ 71.75) (Table 5). More precise information on adaptation costs is still a gap to be met, to promote the application of the alternative adaptive systems (UNEP 2021).

Regarding the quality of recovered water (outflow), an assessment was made based on the resolution CONAMA 357/430 (BRAZIL – MMA 2011), which provides quality standards for water bodies and effluent discharge. Comparing the EMC values over the events with the reference values for water quality of the water bodies, the water recovered from the bioretention was classified as Class 3, for fresh water. Class 3 waters can be destined for human demand supply, after conventional or advanced treatment, irrigation of trees, cereal and forage crops, recreation of secondary contact and animals' consumption. Therefore, it is necessary to improve the water quality before it can be used for NPD-Type1. As for the overflow or excess of

Table 4 | Quantification of water recovery, water stress reduction, and monetary savings for a unitary bioretention system over a typical year

Month	P (mm)	Dry days	Recovered water (m ³)	R\$ saved		WSR	
				NPD-Type1	NPD-Type2	NPD-Type1	NPD-Type2
Jan	320.4	11	23.4	39.9	17.7	0.45	0.20
Feb	233.12	12	17.0	39.9	17.7	0.45	0.20
Mar	175.16	17	12.8	39.9	17.7	0.45	0.20
Apr	89.42	23	6.5	39.9	17.7	0.45	0.20
May	56.19	25	4.1	25.9	17.7	0.29	0.20
Jun	39.45	26	2.9	18.2	17.7	0.20	0.20
Jul	32	28	2.3	14.7	14.7	0.17	0.17
Aug	35.13	27	2.6	16.2	16.2	0.18	0.17
Sep	66.7	23	4.9	30.7	17.7	0.35	0.20
Oct	117.64	21	8.6	39.9	17.7	0.45	0.20
Nov	155.76	18	11.4	39.9	17.7	0.45	0.20
Dec	242.9	14	17.8	39.9	17.7	0.45	0.20

NPD-Type1: Non-potable demands for irrigation and other outdoor uses, flushing toilets and washing machine = 6.3 m³ (per house).

NPD-Type2: Non-potable demands for irrigation and other outdoor uses and flushing toilets = 2.8 m³ (per house).

Dry days: days with 0 mm of precipitation.

Colors – Light red: Deficit for NPD-Type1; Red: Deficit for NPD-Type1 and NPD-Type2.

recovered volume returning to the stream, the water quality agrees with the effluent discharge standards established by the resolution.

For the evaluation on watershed scale, its land use characteristics were raised (Figure 3) to evaluate the reductions in water demands, energy demand and carbon emission, in unitary measurements. Table 5 shows the results obtained for the respective indicators, considering NPD-Type 1 and Type 2. For the indicators presented in this study (WDR, EDR and CER) values as closer to 1 state for better system performance. The use of hybrid systems has a greater impact on the demand for water and energy by the central systems and are able to reduce up to $0.47 \cdot 10^{-6} \text{ m}^3$ of tap water/ $\text{m}^2 A_{\text{bio}}/\text{m}^2 IA_c$ and $0.52 \cdot 10^{-6} \text{ kWh}/\text{m}^2 A_{\text{bio}}/\text{m}^2 IA_c$ in individual systems, during the rainy months when the full capacity of rainwater storage systems is used.

Table 5 | Quantification of the indicators for water demand reduction rates, reduction of energy demand and carbon emissions for the hybrid system in the Mineirinho watershed over a typical year

Month	WDR _{hs}		EDR _{hs}		CER _{hs}		GHG emissions ^a
	NPD-Type1	NPD-Type2	NPD-Type2	NPD-Type1	NPD-Type1	NPD-Type2	
Jan	0.47	0.23	0.52	0.23	0.28	0.12	0.54
Feb	0.47	0.23	0.52	0.23	0.29	0.13	0.56
Mar	0.47	0.23	0.52	0.23	0.28	0.12	0.54
Apr	0.47	0.23	0.52	0.23	0.26	0.12	0.51
May	0.32	0.23	0.34	0.23	0.18	0.12	0.53
Jun	0.24	0.23	0.24	0.23	0.13	0.13	0.56
Jul	0.20	0.20	0.19	0.19	0.11	0.11	0.56
Aug	0.22	0.22	0.21	0.21	0.12	0.12	0.59
Sep	0.37	0.23	0.40	0.23	0.23	0.13	0.58
Oct	0.47	0.23	0.52	0.23	0.30	0.13	0.58
Nov	0.47	0.23	0.52	0.23	0.28	0.12	0.54
Dec	0.47	0.23	0.52	0.23	0.28	0.12	0.54

NPD-Type1: Non-potable demands for irrigation and other outdoor uses, flushing toilets and washing machine = 78,750 m³ (watershed).

NPD-Type2: Non-potable demands for irrigation and other outdoor uses and flushing toilets = 35,000 m³ (watershed).

^aMCTIC (2020).

Conversely, the impacts on carbon emissions are less sensitive, reaching up to $0.28 \cdot 10^{-6} \text{ kgCO}_2/\text{m}^2 A_{\text{bio}}/\text{m}^2 I A_c$. These values establish an initial basis for future comparison with other studies.

4. CONCLUSION

This study evaluated the effect of different configurations of bioretention on their performance regarding flood control and pollutant removal, contributing to SDGs 6, 11 and 13. The statistical tests did not demonstrate significant differences in the efficiencies of runoff retention, peak flow attenuation and water recovery only with USZ and with SZ, however, it was possible to observe a tendency for higher peak flows in the events with SZ. We recommend future evaluations incorporating more extreme chains of events, therefore more representative distributions, to assess whether the SZ leads to large losses in peak flow attenuation efficiency. Conversely, the presence of SZ contributes to improve pollutant removal efficiency. Although it was used to increase the removal of nitrate, favoring the denitrification process, this effect was not noticed, possibly due to the absence of a carbon source in the filtering media. Turbidity, *E. coli* and metals at the outflow were above the limits of the guidelines and standards for freshwater and stormwater reuse in Brazil. Therefore, further studies are necessary to investigate different configurations that improve the treatment process or an additional treatment aimed at solids removal and disinfection. When evaluating the system on the watershed scale, reductions in water demand up to 17.7% were accounted for more restrictive demands, also leading to reductions in energy demand and carbon emission.

FUNDING

This study was supported by an FAPESP grant no. 2014/50848-9 INCT-II (Climate Change, Water Security), CNPq grant no. PQ 312056/2016-8 (EESC-USP/CEMADEN/MCTIC), FAPESP grant no. 2017/15614-5 'Decentralized Urban Runoff Recycling Facility addressing the security of the Water-Energy-Food Nexus', and FAPESP grant no. 2017/26110-8 'A new generation of Sustainable Urban Drainage Systems (SUDS): decentralized and recycling alternatives for the security of water-energy-food nexus'.

DATA AVAILABILITY STATEMENT

All relevant data are included in the paper or its Supplementary Information.

REFERENCES

- ARES-PCJ – Agência Reguladora dos Serviços de Saneamento das Bacias dos Rios Piracicaba, Capivari e Jundiá 2019 *Resolução ARES-PCJ no. 291, de 20 de maio de 2019*. [ARES-PCJ Resolution no. 291, of May 20, 2019]. Available from: <https://www.saaesaocarlos.com.br/docs/ares/2019/20190702resolucao.pdf> (accessed October 2020). (In Portuguese).
- Arnone, E., Pumo, D., Viola, F., Noto, L. V. & La Loggia, G. 2013 *Rainfall statistics changes in Sicily*. *Hydrology and Earth System Sciences* **17** (7), 2449–2458.
- Arora, M., Malano, H., Davidson, B., Nelson, R. & George, B. 2015 *Interactions between centralized and decentralized water systems in urban context: a review*. *Wiley Interdisciplinary Reviews: Water* **2** (6), 623–634.
- Brazil, MMA – Ministério do Meio Ambiente, CONAMA – Conselho Nacional de Meio Ambiente 2011 *Resolução no 430, de 13 de maio de 2011*. [Resolution 430, of May 13, 2011]. Available from: <http://www2.mma.gov.br/port/conama/legiabre.cfm?codlegi=646> (accessed October 2020). (In Portuguese).
- Burns, S., Arnbjerg-Nielsen, K., Hauschild, M. & Rygaard, M. 2015 *The performance of rainwater tanks for stormwater retention and water supply at the household scale: an empirical study*. *Hydrological Processes* **29** (1), 152–160.
- C40 & ARUP 2014 *Climate Action in Megacities: C40 Cities Baseline and Opportunities*. Vol. 2.0. Accessed 2016. Available at http://issuu.com/c40cities/docs/c40_climate_action_in_megacities/149?e=10643095/6541335
- Carter, J. G., Cavan, G., Connelly, A., Guy, S., Handley, J. & Kazmierczak, A. 2015 *Climate change and the city: building capacity for urban adaptation*. *Progress in Planning* **95**, 1–66.
- Chahal, M., Shi, Z. & Flury, M. 2016 *Nutrient leaching and copper speciation in compost-amended bioretention systems*. *Science of the Total Environment* **556**, 302–309.
- Chandrasena, G., Deletic, A. & McCarthy, D. 2016 *Biofiltration for stormwater harvesting: comparison of *Campylobacter* spp. and *Escherichia coli* removal under normal and challenging operational conditions*. *Journal of Hydrology* **537**, 248–259.
- Charalambous, K., Bruggeman, A., Eliades, M., Camera, C. & Vassiliou, L. 2019 *Stormwater retention and reuse at the residential plot level – Green roof experiment and water balance computations for long-term use in Cyprus*. *Water* **11** (5), 1055.
- Charlesworth, S. M. 2010 *A review of the adaptation and mitigation of global climate change using sustainable drainage in cities*. *Journal of Water and Climate Change* **1** (3), 165–180.

- Chou, S. C., Lyra, A., Mourão, C., Dereczynski, C., Pilotto, I., Gomes, J., Bustamante, J., Tavares, P., Silva, A., Rodrigues, D., Campos, D., Chagas, D., Sueiro, G., Siqueira, G. & Marengo, J. 2014 Assessment of climate change over South America under RCP 4.5 and 8.5 downscaling scenarios. *American Journal of Climate Change* **3** (5), 512–525.
- D'Acunha, B. & Johnson, M. 2019 Water quality and greenhouse gas fluxes for stormwater detained in a constructed wetland. *Journal of Environmental Management* **231**, 1232–1240.
- Davis, A. P., Shokouhian, M., Sharma, H. & Minami, C. 2006 Water quality improvement through bioretention media: nitrogen and phosphorus removal. *Water Environmental Research* **78** (3), 284–293.
- Eckart, K., McPhee, Z. & Bolisetti, T. 2017 Performance and implementation of low impact development – a review. *Science of The Total Environment* **607**, 413–432.
- Escobar, H. 2015 Drought triggers alarms in Brazil's biggest metropolis. *Science* **347** (6224), 812–812.
- Fletcher, T., Andrieu, H. & Hamel, P. 2013 Understanding, management and modelling of urban hydrology and its consequences for receiving waters: a state of the art. *Advances in Water Resources* **51**, 261–279.
- Fletcher, T., Shuster, W., Hunt, W., Ashley, R., Butler, D., Arthur, S. & Mikkelsen, P. 2015 SUDS, LID, BMPs, WSUD and more – The evolution and application of terminology surrounding urban drainage. *Urban Water Journal* **12** (7), 525–542.
- Freni, G. & Liuzzo, L. 2019 Effectiveness of rainwater harvesting systems for flood reduction in residential urban areas. *Water* **11** (7), 1389.
- Ge, Z., Feng, C., Wang, X. & Zhang, J. 2016 Seasonal applicability of three vegetation constructed floating treatment wetlands for nutrient removal and harvesting strategy in urban stormwater retention ponds. *International Biodeterioration & Biodegradation* **112**, 80–87.
- Getter, K., Rowe, D., Robertson, G., Cregg, B. & Andresen, J. 2009 Carbon sequestration potential of extensive green roofs. *Environmental Science & Technology* **43** (19), 7564–7570.
- Gomes Junior, M. N. 2019 Aspectos hidrológicos-hidráulicos e avaliação de eficiência de biorretenções: Modelos, princípios e critérios de projeto de técnicas compensatórias de 3ª geração. [Hydrological-Hydraulic Aspects and Efficiency Assessment of Bioretentions: Models, Principles and Design Criteria for Third Generation LID]. Master Thesis, University of São Paulo, São Carlos School of Engineering, Department of Hydraulic and Sanitation (in Portuguese).
- Hansen, J., Ruedy, R., Sato, M. & Lo, K. 2010 Global surface temperature change. *Reviews of Geophysics* **48**, 4.
- Hashemi, S., Mahmud, H. & Ashraf, M. 2015 Performance of green roofs with respect to water quality and reduction of energy consumption in tropics: a review. *Renewable and Sustainable Energy Reviews* **52**, 669–679.
- Helsel, D. R., Hirsch, R. M., Ryberg, K. R., Archfield, S. A. & Gilroy, E. J. 2020 *Statistical Methods in Water Resources: U.S. Geological Survey Techniques and Methods, Book 4, Chapter A3*, p. 458. [Supersedes USGS Techniques of Water-Resources Investigations, book 4, chapter A3, version 1.1.]. <https://doi.org/10.3133/tm4a3>.
- IPCC 2007 *Contribution of Working Groups I, II and III to the Fourth Assessment Report of the Intergovernmental Panel on Climate Change*. Geneva, Switzerland, p. 104.
- Jones, J., Clary, J., Strecker, E. & Quigley, M. 2008 15 reasons why you should think twice before using percent removal to assess BMP performance. *Stormwater*, 9, Guest Editorial, January/February. https://www.researchgate.net/publication/280843991_15_Reasons_You_Should_Think_Twice_before_Using_Percent_Removal_to_Assess_BMP_Performance
- Kim, H., Seagren, E. A. & Davis, A. P. 2003 Engineered bioretention for removal of nitrate from stormwater runoff. *Water Environment Research* **75** (4), 355–367.
- Lago, C. A. F., Macedo, M. B., Rosa, A. & Mendiondo, E. M. 2017 Calibração e validação quali-quantitativa do escoamento superficial – Estudo de caso na USP/São Carlos. [Calibration and quali-quantitative validation of runoff – Case study at USP/São Carlos]. In: *Proceedings of XXII Simpósio Brasileiro de Recursos Hídricos*, 2017, Florianópolis (In Portuguese).
- Laurenson, G., Laurenson, S., Bolan, N., Beechan, S. & Clark, I. 2013 The role of bioretention systems in the treatment of stormwater. *Advances in Agronomy*. **120**, 223–274.
- Liuzzo, L., Noto, L. V., Arnone, E., Caracciolo, D. & La Loggia, G. 2015 Modifications in water resources availability under climate changes: a case study in a Sicilian Basin. *Water Resources Management* **29** (4), 1117–1135.
- Lyra, A., Tavares, P., Chou, S. C., Sueiro, G., Dereczynski, C., Sondermann, M., Silva, A., Marengo, J. & Giarolla, A. 2018 Climate change projections over three metropolitan regions in Southeast Brazil using the non-hydrostatic Eta regional climate model at 5-km resolution. *Theoretical and Applied Climatology* **132** (1–2), 663–682.
- Macedo, M. B., Lago, C. A. F., Mendiondo, E. M. & Souza, V. C. B. 2018 Performance of bioretention experimental devices: contrasting laboratory and field scales through controlled experiments. *RBRH* **23**, e3.
- Macedo, M. B., Lago, C. A. F. & Mendiondo, E. 2019a Stormwater volume reduction and water quality improvement by bioretention: potentials and challenges for water security in a subtropical catchment. *Science of the Total Environment* **647**, 923–931.
- Macedo, M. B., Lago, C. A. F., Mendiondo, E. & Giacomoni, M. 2019b Bioretention performance under different rainfall regimes in subtropical. *Journal of Environmental Management* **248**, 109266.
- Macedo, M. B., Gomes Junior, M. N., Oliveira, T. R. P., Giacomoni, M. H., Imani, M., Zhang, K., Lago, C. A. F. & Mendiondo, E. M. 2021 Low impact development practices in the context of united nations sustainable development goals: a new concept, lessons learned and challenges. *Critical Reviews in Environmental Science and Technology*. DOI: 10.1080/10643389.2021.1886889.
- Mangangka, I., Liu, A., Egodawatta, P. & Goonetilleke, A. 2015 Performance characterization of a stormwater treatment bioretention basin. *Journal of Environment Management* **150**, 173–178.

- MCTIC – Ministério da Ciência Tecnologia e Inovações 2020 *Arquivos dos Fatores de Emissão da Margem de Operação Pelo Método da Análise de Despacho. [Operating Margin Emission Factors Files by Dispatch Analysis Method]*. Available from: http://antigo.mctic.gov.br/mctic/opencms/ciencia/SEPED/clima/textogeral/emissao_despacho.html (accessed October 2020). (In Portuguese).
- Miller, J. D. & Hutchins, M. 2017 The impacts of urbanisation and climate change on urban flooding and urban water quality: a review of the evidence concerning the United Kingdom. *Journal of Hydrology: Regional Studies* **12**, 345–362.
- Nair, S., George, B., Malano, H., Arora, M. & Nawarathna, B. 2014 *Water–energy–greenhouse gas nexus of urban water systems: review of concepts, state-of-art and methods*. *Resources, Conservation and Recycling* **89**, 1–10.
- Ng, K., Herrero, P., Hatt, B., Farrelly, M. & McCarthy, D. 2018 Biofilters for urban agriculture: metal uptake of vegetables irrigated with stormwater. *Ecological Engineering* **122**, 177–186.
- Payne, E. G. I., Pham, T., Cook, P. L. M., Fletcher, T. D., Hatt, B. E. & Deletic, A. 2014a *Biofilter design for effective nitrogen removal from stormwater–influence of plant species, inflow hydrology and use of a saturated zone*. *Water Science and Technology* **69** (6), 1312–1319.
- Payne, E. G., Fletcher, T. D., Russell, D. G., Grace, M. R., Cavagnaro, T. R., Evrard, V., Deletic, A., Hatt, B. E. & Cook, P. L. M. 2014b *Temporary storage or permanent removal? The division of nitrogen between biotic assimilation and denitrification in stormwater biofiltration systems*. *PLoS One* **9** (3), e90890.
- Pedregosa, F., Varoquaux, G., Gramfort, A., Michel, V., Thirion, B., Grisel, O. & Vanderplas, J. 2011 Scikit-learn: Machine learning in Python. *Journal of Machine Learning Research* **12**, 2825–2830. Available from: <http://jmlr.org/papers/v12/pedregosa11a.html>.
- Petit-Boix, A., Deykota, J., Phillips, R., VargasParra, M., Josa, A., Gabarrell, X. & Apul, D. 2018 *Life cycle and hydrologic modeling of rainwater harvesting in urban neighborhoods: implications of urban form and water demand patterns in the US and Spain*. *Science of the Total Environment* **621**, 434–443.
- PyPi 2019 *Scikit-posthocs 0.6.1*. Available from: <https://pypi.org/project/scikit-posthocs/0.6.1/>.
- PyPi 2020a *SciPy 1.5.0*. Available from: <https://pypi.org/project/scipy/1.5.0/>.
- PyPi 2020b *Scikit-learn 0.23.2*. Available from: <https://pypi.org/project/scikit-learn/0.23.2/>.
- Richards, R. C., Rerolle, J., Aronson, J., Pereira, P. H., Gonçalves, H. & Brancalion, P. H. S. 2015 *Governing a pioneer program on payment for watershed services: stakeholder involvement, legal frameworks and early lessons from the Atlantic forest of Brazil*. *Ecosystem Services: Science, Policy and Practice* **16**, 23–32.
- Roy-Poirier, A., Champagne, P. & Filion, Y. 2010 *Bioretention processes for phosphorus pollution control*. *Environmental Reviews* **18** (NA), 159–173.
- Sambito, M., Severino, A., Freni, G. & Neduzha, L. 2021 *A systematic review of the hydrological, environmental and durability performance of permeable pavement systems*. *Sustainability* **13** (8), 4509.
- Sapkota, M., Arora, M., Malano, H., Moglia, M., Sharma, A., George, B. & Pamminer, F. 2015 *An overview of hybrid water supply systems in the context of urban water management: challenges and opportunities*. *Water* **7** (1), 153–174.
- Shen, P., Deletic, A., Urich, C., Chandrasena, G. I. & McCarthy, D. T. 2018 *Stormwater biofilter treatment model for faecal microorganisms*. *Science of the Total Environment* **630**, 992–1002.
- SNIS – Sistema Nacional de Informações sobre Saneamento 2018 *Série Histórica. [Historical Serie]*. Available from: <http://app4.mdr.gov.br/serieHistorica/> (accessed October 2020).
- Søberg, L. C., Viklander, M., Blecken, G. T. & Hedström, A. 2019 *Reduction of Escherichia coli, Enterococcus faecalis and Pseudomonas aeruginosa in stormwater bioretention: effect of drying, temperature and submerged zone*. *Journal of Hydrology X* **3**, 100025.
- Stott, R., Tondera, K., Blecken, G. T. & Schreiber, C. 2017 *Microbial loads and removal efficiency under varying flows*. In: Tondera, K., Blecken, G. T., Chazarenc, F. & Tanner, C. C. (eds). *Ecotechnologies for the Treatment of Variable Stormwater and Wastewater Flows*. Springer, Cham, pp. 57–74.
- Tafarello, D., Mohor, G. S., Calijuri, M. C. & Mendiondo, E. M. 2016 *Field investigations of the 2013–14 drought through quali-quantitative freshwater monitoring at the headwaters of the Cantareira System, Brazil*. *Water International* **41** (5), 776–800.
- UNEP – United Nations Environment Programme 2021 *Adaptation Gap Report 2020 – Online Annex*. UNEP-DTU-WASP, Nairobi. ISBN: 978-92-807-3834-6.
- UNSTATS 2020 *Global indicator framework adopted by the General Assembly (A/RES/71/313)*, annual refinements contained in E/CN.3/2018/2 (Annex II), E/CN.3/2019/2 (Annex II), and 2020 Comprehensive Review changes (Annex II) and annual refinements (Annex III) contained in E/CN.3/2020/2. Available from: <https://unstats.un.org/sdgs/indicators/indicators-list/> (accessed October 2020).
- UN – United Nations 2020 *The 17 Goals*. Available from: <https://sdgs.un.org/goals> (accessed October 2020).
- Virtanen, P., Gommers, R., Oliphant, T. E., Haberland, M., Reddy, T., Cournapeau, D., Burovski, E., Peterson, P., Weckesser, W., Bright, J., van der Walt, S. J., Brett, M., Wilson, J., Millman, K. J., Mayorov, N., Nelson, A. R. J., Jones, E., Kern, R., Larson, E., Carey, C. J., Polat, I., Feng, Y., Moore, E. W., VanderPlas, J., Laxalde, D., Perktold, J., Cimrman, R., Henriksen, I., Quintero, E. A., Harris, C. R., Archibald, A. M., Ribeiro, A. H., Pedregosa, F. & van Mulbregt, P. 2020 *SciPy 1.0: fundamental algorithms for scientific computing in Python*. *Nature Methods* **17** (3), 261–272.
- WWEGC – Wright Water Engineers and Geosyntec Consultants 2007 *Frequently Asked Questions Fact Sheet for the International Stormwater BMP Database: Why does the International Stormwater BMP Database Project omit percent removal as a measure of BMP performance?* (as posted on www.bmpdatabase.org).